Acta Crystallographica Section D
**Biological Crystallography**
ISSN 0907-4449

# Crystallization and preliminary crystallographic analysis of the autoinhibited form of the tandem SH3 domain of p47$^{phox}$

**Satoru Yuzawa,[a,b] Nobuo N. Suzuki,[a,b] Yuko Fujioka,[a,b] Kenji Ogura,[a,b] Hideki Sumimoto[c] and Fuyuhiko Inagaki[a,b]***

[a]Department of Structural Biology, Graduate School of Pharmaceutical Sciences, Hokkaido University, Sapporo 060-0812, Japan, [b]CREST, Japan Science and Technology Corporation, 4-1-8 Honmachi, Kawaguchi 332-0012, Japan, and [c]Medical Institute of Bioregulation, Kyushu University, Fukuoka 812-8582, Japan

Correspondence e-mail: finagaki@pharm.hokudai.ac.jp

Received 6 February 2003
Accepted 27 May 2003

p47$^{phox}$ is a cytosolic component of the phagocyte NADPH oxidase, which is responsible for the production of the superoxide which kills invasive microorgamisms. A recombinant form of a histidine-tagged tandem SH3 domain of the p47$^{phox}$-containing polybasic autoinhibited region was expressed in *Escherichia coli* and purified and crystallized by the sitting-drop vapour-diffusion method at 293 K using polyethylene glycol 6000 as a precipitant. Diffraction data were collected to 2.15 Å resolution at 100 K using synchrotron radiation. The crystal belongs to space group $P4_12_12$ or $P4_32_12$, with unit-cell parameters $a = 100.02$, $c = 44.94$ Å. The presence of one molecule per asymmetric unit gives a crystal volume per protein mass ($V_M$) of 2.6 Å$^3$ Da$^{-1}$ and a solvent content of 52% by volume.

## 1. Introduction

The NADPH oxidase of neutrophils and other phagocytic cells plays a critical role in the host defence system against microbial infection and catalyses the reduction of oxygen to superoxide using NADPH as an electron donor. The phagocyte NADPH oxidase is a multicomponent enzyme comprising a membrane-bound flavocytochrome $b_{558}$, which is a heterodimer of gp91$^{phox}$ and p22$^{phox}$, and at least four cytosolic regulatory subunits consisting of p47$^{phox}$, p67$^{phox}$, p40$^{phox}$ and Rac (reviewed in Babior, 1999). In the resting state, the oxidase subunits are localized separately at the membrane and cytoplasm. Recently, p47$^{phox}$, p67$^{phox}$ and p40$^{phox}$ were found to form a complex with 1:1:1 stoichiometry by analytical ultracentrifugation analysis (Lapouge *et al.*, 2002). Upon activation of the cell, the p47$^{phox}$–p67$^{phox}$–p40$^{phox}$ complex translocates from the cytosol to the plasma membrane and associates with flavocytochrome $b_{558}$, which generates superoxide. This translocation process is initiated by a series of tighly regulated signalling events to assemble the NADPH oxidase subunits into the activated complex. p47$^{phox}$ has a key role in this process and contains a PX domain, a tandem SH3 domain, a polybasic region and a proline-rich region in that order. In the inactive state, the tandem SH3 domain of p47$^{phox}$ is masked owing to an intramolecular interaction with the polybasic region, resulting in the autoinhibited form (Sumimoto *et al.*, 1996; Hata *et al.*, 1998). Upon cell stimulation, some serine residues of p47$^{phox}$ are phosphorylated (el Benna *et al.*, 1994), which triggers activation of the NADPH oxidase (Inanami *et al.*, 1998; Ago *et al.*, 1999), possibly arising from conformational changes that subsequently lead to rearrangements of the intramolecular interactions (Swain *et al.*, 1997; Ago *et al.*, 1999). Thus, the tandem SH3 domain of p47$^{phox}$ is unmasked and capable of binding to a cytoplasmic proline-rich region of p22$^{phox}$ (Leto *et al.*, 1994; Sumimoto *et al.*, 1994). This interaction is considered to be essential for NADPH oxidase activation (de Mendez *et al.*, 1996; Sumimoto *et al.*, 1996).

To elucidate the masking mechanism of the tandem SH3 domain of p47$^{phox}$ based on its tertiary structure, we have initiated a crystallographic analysis of p47$^{phox}$ in the autoinhibited form. Here, we report the purification, crystallization and preliminary X-ray crystallographic analysis of the autoinhibited tandem SH3 domain.

## 2. Materials and methods

### 2.1. Expression and purification

The autoinhibited form of the tandem SH3 domain of p47$^{phox}$ [amino-acid residues 151–340, abbreviated p47$^{phox}$(151–340)] has been chosen for crystallographic studies; it contains the tandem SH3 domain and the polybasic region. p47$^{phox}$(151–340) was not able to interact with a cytoplasmic proline-rich region of p22$^{phox}$, but could be induced to bind p22$^{phox}$ upon addition of arachidonic acid and SDS (data not shown).

The DNA sequence encoding p47$^{phox}$(151–340) was cloned into vector pPro EX HTb (Invitrogen). The polyhistidine-tagged p47*phox*(151–340) was overexpressed in *Escherichia coli* BL21(DE3). The cells were disrupted by sonication at 277 K in 25 m*M* Tris buffer at pH 7.8 and 500 m*M* NaCl. The protein was applied onto an Ni–NTA (Qiagen) column equilibrated with 25 m*M* Tris buffer pH 7.8, 500 m*M* NaCl and 5 m*M* imidazole.

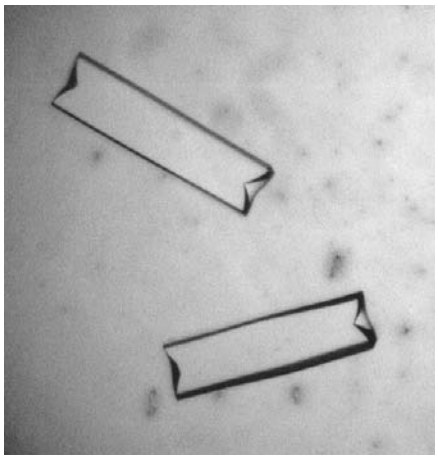

**Figure 1**
Single crystal of human p47$^{phox}$(151–340). The maximum dimensions of the crystal in this photograph are 0.35 × 0.1 × 0.05 mm.

The bound protein was eluted with 25 m*M* Tris buffer pH 7.8, 500 m*M* NaCl and 250 m*M* imidazole. Fractions containing protein were purified on a Superdex 75 gel-filtration column (Amersham Biosciences) and eluted with 25 m*M* potassium phosphate buffer pH 6.5 and 150 m*M* NaCl. The N-terminal histidine tag of p47$^{phox}$(151–340) was then removed by incubation with TEV protease (Gibco BRL) for 12 h at 293 K and the digested protein was dialyzed against 2 l of 25 m*M* potassium phosphate buffer pH 6.5. The protein was purified on a CM Sepharose Fast Flow 5 ml column (Amersham Biosciences) equilibrated with 25 m*M* potassium phosphate buffer pH 6.5 and the protein was eluted with a 0–500 m*M* NaCl gradient in the same buffer. Further purification was carried out on a Superdex 75 gel-filtration column (Amersham Biosciences) eluted with 25 m*M* bis-tris buffer pH 6.5 and 150 m*M* NaCl. The protein was concentrated by Centriprep YM-10 (Millipore) to around 30 mg ml$^{-1}$.

### 2.2. Crystallization and data collection

Crystallization was performed at 293 K by the sitting-drop vapour-diffusion method using a 96-well sitting-drop plate (Hampton Research). The drops contained 0.5 µl of reservoir solution and 0.5 µl of 25–35 mg ml$^{-1}$ protein and were equilibrated against 100 µl of reservoir solution. Initial trials were performed with a sparse-matrix system (Jancarik & Kim, 1991) using screening kits from Hampton Research and Emerald BioStructures. Initially, small crystals were grown from solution No. 6 [100 m*M* citrate pH 5.5, 20%(*w*/*v*) PEG 3000, final pH 6.0] of the Wizard I screening kit (Emerald BioStructures) in about two months. The best crystals were grown in the presence of 50 m*M* sodium fluoride at 293 K in a reservoir solution containing 100 m*M* sodium citrate pH 5.4–5.6 and 16–18% polyethylene glycol 6000 (Hampton Research). Crystals grew within one month to average dimensions of approximately 0.3 × 0.2 × 0.05 mm (Fig. 1).

**Table 1**
Crystallographic parameters and data-collection statistics.

Values in parentheses indicate statistics for the highest resolution shell (2.23–2.15 Å).

| | |
|---|---|
| Space group | $P4_12_12$ or $P4_32_12$ |
| Unit-cell parameters (Å) | $a = b = 100.02$, $c = 44.94$ |
| Mathews coefficient (Å$^3$ Da$^{-1}$) | 2.6 (1 molecule per AU) |
| Solvent content (%) | 52 |
| Resolution range (Å) | 50.0–2.15 (2.23–2.15) |
| Observed reflections | 106951 |
| Unique reflections | 12740 |
| Average $I/\sigma(I)$ | 10.3 (5.4) |
| $R_{merge}$† (%) | 6.9 (23.1) |
| Completeness (%) | 98.3 (99.8) |
| Redundancy | 8.4 |

For data collection, crystals were mounted in nylon loops (Hampton Research) after soaking in a cryoprotectant solution (25% polyethylene glycol 6000, 100 m*M* sodium citrate pH 6.0, 7% glycerol). The crystals were then flash-frozen in a nitrogen stream at 100 K. Diffraction data were collected at the BL41XU beamline, SPring-8 (Harima, Japan) using a wavelength of 0.980 Å and a crystal-to-detector distance of 150 mm. Diffraction intensity was measured using a MAR CCD 165 detector with 10 s exposures. Diffraction data were collected from 120 images using the oscillation method; individual frames consisted of 1.0° oscillation steps over a range of 120°. All data sets were processed and scaled using the *HKL*2000 program package (Otwinowski & Minor, 1997).

## 3. Results

The crystal of p47$^{phox}$(151–340) belongs to the tetragonal space group $P4_12_12$ or $P4_32_12$, with unit-cell parameters $a = b = 100.02$, $c = 44.94$ Å and a resultant unit-cell volume of 449 600 Å$^3$. A nearly complete data set was collected to 2.15 Å resolution. Assuming one p47$^{phox}$(151-–340) molecule (MW = 21 989 Da) to be present in the asymmetric unit, the Matthews coefficient ($V_M$) was calculated to be 2.56 Å$^3$ Da$^{-1}$, which is within the expected range (Matthews, 1968). This $V_M$ value corresponds to a solvent content of approximately 52%. The crystallographic parameters and data-collection statistics are shown in Table 1. 106 951 observed reflections were reduced to 12 740 unique reflections, with an overall $R_{merge}$ of 6.9% and an overall $I/\sigma(I)$ of 10.3. This represents 98.3% of the theoretically observable reflections for the resolution range 50–2.15 Å.

The sequence of p47$^{phox}$(151–340) contains four methionine residues. We have produced crystals of the selenomethionine (SeMet) substituted protein and confirmed proper incorporation of SeMet by mass spectroscopy. We are currently optimizing crystallization conditions for SeMet crystals of p47$^{phox}$(151–340) for use in the MAD method (Hendrikson *et al.*, 1990).

This work was supported by CREST, Japan Science and Technology (JST) and by a Grant-in-Aid for Scientific Research on Priority Areas from the Japan Ministry of Education, Science and Culture.

## References

Ago, T., Nunoi, H., Ito, T. & Sumimoto, H. (1999). *J. Biol. Chem.* **274**, 33644–33653.
Babior, B. M. (1999). *Blood*, **93**, 1464–1476.
Benna, J. el, Faust, L.P. & Babior, B. M. (1994). *J. Biol. Chem.* **269**, 23431–23436.
Hata, K., Ito, T., Takeshige, K. & Sumimoto, H. (1998). *J. Biol. Chem.* **273**, 4232–4236.
Hendrikson, W. A., Horton, J. R. & LeMaster, D. M. (1990). *EMBO J.* **9**, 1665–1672.
Inanami, O., Jonson, J. T., McAdara, J. K., el Benna, J., Faust, L. P., Newburger, P. E. & Babior, B. M. (1998). *J. Biol. Chem.* **273**, 9539–9543.
Jancarik, J., & Kim, S.-H. (1991). *J. Appl. Cryst.* **24**, 409–411.
Lapouge, K., Smith, S. J., Groemping, Y. & Rittinger, K. (2002). *J. Biol. Chem.* **277**, 10121–10128.
Leto, T. L., Adams, A. G. & de Mendez, I. (1994). *Proc. Natl Acad. Sci. USA*, **91**, 10650–10654.
Matthews, B. W. (1968). *J. Mol. Biol.* **33**, 491–497.
Mendez, I. de, Adams, A. G., Sokolic, R. A., Malech, H. L. & Leto, T. L. (1996). *EMBO J.* **15**, 1211–1220.
Otwinowski, W. & Minor, W. (1997). *Methods Enzymol.* **276**, 307–326.
Sumimoto, H., Hata, K., Mizuki, K., Ito, T., Kage, Y., Sakaki, Y., Fukumaki, Y., Nakamura, M. & Takeshige, K. (1996). *J. Biol. Chem.* **271**, 22152–22158.
Sumimoto, H., Kage, Y., Nunoi, H., Sasaki, H., Nose, T., Fukumaki, Y., Ohno, M., Minakami, S. & Takeshige, K. (1994). *Proc. Natl Acad. Sci. USA*, **91**, 5345–5349.
Swain, D. S., Helgerson, S. L., Davis, A. R., Nelson, L. K. & Quinn, M. T. (1997). *J. Biol. Chem.* **272**, 29502–29510.